Theoretical Study of Electronic Structures and Spectra of Chalcogenido Complexes of Molybdenum, *trans*-$Mo(Q)_2(PH_3)_4$ (Q = O, S, Se, Te)

F. Albert Cotton* and Xuejun Feng

Department of Chemistry and Laboratory for Molecular Structure and Bonding, Texas A&M University, College Station, Texas 77843-3255

Received September 28, 1995[⊗]

Electronic structures of the title complexes have been studied using quantum chemical computations by different methods. It is shown that the results of Xα calculations agree well with expectations from classical ligand-field theory, but both are far from being in agreement with the results given by *ab initio* calculations. The HOMO in the *ab initio* Hartree−Fock molecular orbital diagrams of all these complexes is a chalcogen p_π lone pair orbital rather than the metal nonbonding d_{xy} orbital previously proposed. Electronic transition energies were calculated by CASSCF and CI methods. The results suggest that in the cases when Q = S, Se, and Te the lowest energy transitions should be those from the p_π lone pair orbitals to the metal−chalcogen π^* orbitals. The calculated and observed electronic spectra of the oxo complex are in good agreement and very different from the spectra of the other complexes, and the lowest absorptions were accordingly assigned to transitions of different origins.

Introduction

The chemistry of transition-metal complexes that contain multiple bonds between a metal atom and ligands has been extensively explored in recent years.[1,2] Efforts in synthesis and characterization have led to production of a great number of such complexes of many different structural types.[1,2] Among them are a special structural group, namely, the terminal chalcogenido complexes of general formula *trans*-$M(Q)_2L_4$ (Q = O, S, Se, Te). These complexes have the geometry of a flattened octahedron, with the two chalcogen atoms trans to each other and both doubly bonded to the central metal atom. Within this group, the *trans*-dioxo complexes have been the most studied species with regard to their synthesis, reactions, molecular structrues, and spectroscopic properties,[1−3] whereas the sulfido,[4] selenido, and tellurido complexes are relatively new contributions among the latest developments in the field. The first tellurido complex,[5] *trans*-$W(Te)_2(PMe_3)_4$, as well as its sulfur analogue[6] was reported recently by Parkin and co-workers. Very recently, Parkin and co-workers published syntheses and crystal structures of a similar series of chalcogenido complexes of molybdenum, namely, *trans*-$Mo(Q)_2(PMe_3)_4$ (Q = S, Se, Te).[7]

The electronic structures of the metal−chalcogen multiply bonded complexes have also been studied by both experimental and theoretical methods. Electronic spectra of some these complexes have been measured and reported. Among them the dioxo complexes, in particular the *trans*-dioxorhenium complexes,[3] were extensively studied. A study of the electronic structures and absorption spectra of the *trans*-$W(Q)_2(PMe_3)_4$ (Q = S, Se, Te) complexes was reported recently.[8] Only a few other theoretical studies have been reported for complexes of this type. In some cases observed electronic spectra have been discussed only on the basis of qualitative ligand-field theory,[3,8] although molecular orbital calculations by the DV−Xα method were reported recently for a series of tungsten complexes, namely, $W(Q)_2(PH_3)_4$ (Q = O, S, Te).[9] The general features of electronic structure and bonding as described by these calculations are similar to what one would expect from the ligand field theory by considering an axially compressed octahedral ligand field around the metal center.[10] There are also *ab initio* calculations reported recently for the tungsten complexes, but only molecular geometry optimization was considered within the Hartree−Fock approximation.[11]

In this laboratory, we have been pursuing an extensive investigation of metal−chalcogen multiple bonds by both experimental and theoretical means. With synthetic approaches different from those in literature, we have obtained a complete series of complexes containing chalcogen-molybdenum multiple bonds,[12] namely, *trans*-$Mo(Q)_2(PP)_2$, where Q = O, S, Se, and Te and PP is a chelating bidentate phosphine ligand, $Ph_2PCH{=}CHPPh_2$ (dppee) or $Ph_2PCH_2CH_2PPh_2$ (dppe). All these complexes have been characterized by X-ray crystallographic and various spectroscopic methods.[12] We have also carried out systematic studies on the electronic structures of these complexes employing different types of quantum chemical computation. We report in this paper the results of our calculations on a series of model compounds, namely, $Mo(Q)_2(PH_3)_4$ (Q = O, S, Se, Te). We will discuss the electronic structures of these molecules in their ground state in terms of molecular orbital diagrams calculated by the SCF−Xα−SW molecular orbital method and the *ab initio* Hartree−Fock method. Further discussion of electronic transitions will be given on the basis of *ab initio* CASSCF and CI calculations for both ground and excited states.

[⊗] Abstract published in *Advance ACS Abstracts,* August 1, 1996.

(1) Nugent, W. A.; Mayer, J. M. *Metal-Ligand Multiple Bonds*; Wiley: New York, 1988.
(2) Holm, R. H. *Chem. Rev.* **1987**, *87*, 1401.
(3) (a) Winkler, J. R.; Gray, H. B. *Inorg. Chem.* **1985**, *24*, 346. (b) Brewer, J. C.; Thorp, H. H.; Slagle, K. M.; Brudvig, G. W.; Gray, H. B. *J. Am. Chem. Soc.* **1991**, *113*, 3171.
(4) Yoshida, T.; Adachi, T.; Matsumura, K.; Kawazu, K.; Baba, K. *Chem. Lett.* **1991** 1067.
(5) Rabinovich, D.; Parkin, G. *J. Am. Chem. Soc.* **1991**, *113*, 9421.
(6) Rabinovich, D.; Parkin, G. *J. Am. Chem. Soc.* **1991**, *113*, 5904.
(7) Murphy, V. J.; Parkin, G. *J. Am. Chem. Soc.* **1995**, *117*, 3522.
(8) Paradis, J. A.; Wertz, D. W.; Thorp, H. H. *J. Am. Chem. Soc.* **1993**, *115*, 5308.
(9) Kaltsoyannis, K. *J. Chem. Soc., Dalton Trans.* **1994**, 1391.
(10) Ballhausen, C. J.; Gray, H. B. *Inorg. Chem.* **1962**, *1*, 111.
(11) Benson, M. T.; Cundari, T. R.; Lim, S. J.; Nguyen, H. D.; Pierce-Beaver, K. *J. Am. Chem. Soc.* **1994**, *116*, 3955.
(12) Cotton, F. A.; Schmid, G., To be submitted for publication.

S0020-1669(95)01261-4 CCC: $12.00

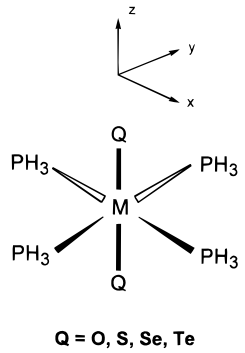

Figure 1. Model for calculations.

Computational Details

The model compounds to be calculated are shown in Figure 1. While the highest possible molecular symmetry of a MQ_2L_4 type of complex is D_{4h}, because of the phosphine ligands, the highest symmetry of *trans*-$Mo(Q)_2(PH_3)_4$ may only be as high as C_{4v}, D_{2d}, or D_{2h}, depending on the orientation of the hydrogen atoms in the PH_3 ligand. We chose D_{2h} symmetry for the present computational studies because all important metrical parameters used in the calculations were obtained from crystal structure data[12] of the $Mo(Q)_2(dppee)_2$ complexes which have virtual D_{2h} symmetry. The bond distances and angles are Mo−O = 1.80 Å, Mo−S = 2.24 Å, Mo−Se = 2.38 Å, Mo−Te = 2.60 Å, Mo−P = 2.52 Å, and Q−Mo−P = P-Mo-P = 90°, and P-H was chosen to be 1.42 Å. For the purpose of comparison, two tungsten compounds in D_{2d} symmetry, namely, $W(S)_2(PH_3)_4$ (W−S = 2.30 Å, W−P = 2.52 Å) and $W(Te)_2(PH_3)_4$ (W−Te = 2.60 Å, W−P = 2.52 Å), were also calculated. They are the models for the D_{2d} *trans*-$W(Q)_2(PMe_3)_4$ complexes.[5]

The *ab initio* calculations utilized effective core potentials (ECP) so that only the outermost electrons of each atom were treated explicitly. For the metal atoms, these include electrons in the *n*s, *n*p, *n*d, and (*n* + 1)s orbitals, and for the main group atoms these are *n*s and *n*p electrons. We used the ECPs of Hay and Wadt[13] that include relativistic effects for elements with $Z > 36$, and their valence Gaussian basis sets for Mo, W, S, Se, Te, and P, and the compact effective potential and basis functions due to Stevens *et al*. for the oxygen atom.[14] The (5s5p4d) basis set for Mo and the (5s5p3d) set for W were contracted to a (3s3p3d) set, and for the main group elements, the final contracted basis sets (2s2p) are all of double-ζ quality. The basis sets for the chalcogens were also augmented with a d polarization function of exponent 0.85, 0.54, 0.25, and 0.15, repectively, for O, S, Se, and Te. For the purpose of comparison, all-electron Hartree−Fock calculations were also performed for the $Mo(O)_2(PH_3)_4$ and $Mo(S)_2(PH_3)_4$ complexes. The basis sets for these calculations are a (10s8p5d) basis set for Mo contracted from the (15s9p8d) set plus two diffuse p functions and one diffuse d function of Veillard and Dedieu[15] and full double-ζ basis sets[16] for H, O, S, and P plus a d polarization function for O and S.

The ground state of each compound was calculated at both restricted Hartree−Fock (RHF) and complete active space self-consistent-field (CASSCF) levels. The active orbital space from which the CASSCF wave functions were constructed will be discussed later in detail. The CASSCF calculations were also carried out for the lowest excited state of each given space and spin symmetry. Excited states that have the same space and spin symmetry as the lowest state were determined by full CI calculations in the orbital space of the same size but optimized for the CASSCF lowest state. The calculations employed the program GAMESS[17] and the CASSCF calculations were accomplished by the MCSCF module[18] in the program.

(13) Hay, P. J.; Wadt, W. R. *J. Chem. Phys*. **1985**, *82*, 270, 284, and 299.
(14) Stevens, W. J.; Basch, H.; Krauss, M. *J. Chem. Phys*. **1984**, *81*, 6026.
(15) Veillard, A.; Dedieu, A. *Theor. Chim. Acta* **1984**, *65*, 215.
(16) Dunning Jr., T. H. *J. Chem. Phys*. **1970**, *53*, 2823.
(17) Guest, M. F. *GAMESS User's Guide and Reference Manual*; Daresbury Laboratory: Daresbury, U.K., 1989.
(18) Knowles, P. J.; Werner, H. *J. Chem. Phys. Lett*. **1985**, *115*, 259.

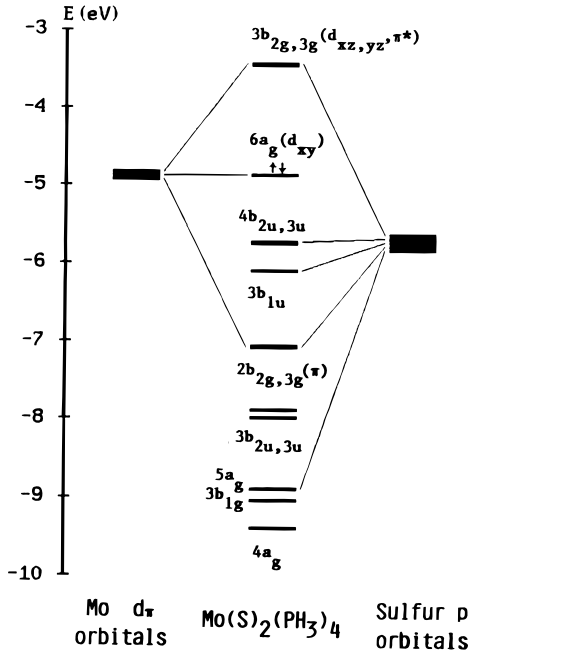

Figure 2. Upper valence molecular orbitals for $Mo(S)_2(PH_3)_4$ with D_{2h} symmetry calculated by the SCF−Xα−SW method. Energies of metal d_π orbitals and sulfur p orbitals were set arbitrarily.

Results and Discussion

Ground State Electronic Structure. Qualitatively, the electronic structure of a d^2 complex of the type shown in Figure 1 may be described in terms of splitting of the metal d orbitals in the field of an octahedron distorted by axial compression.[10] In the case of full O_h symmetry, the five d orbitals split into a degenerate e_g ($d_{x^2-y^2}$, d_{z^2}) set of Mo−P and Mo−Q σ antibonding character and a nonbonding t_{2g} (d_{xy}, d_{xz}, d_{yz}) set. When the axial ligands (on the *Z* axis) are replaced by a pair of π bonding ligands the molecular symmetry is lowered and both e_g and t_{2g} orbitals are split further. Quantitatively, we do not expect a large split for the e_g set (a_{1g} and b_{1g} in D_{4h}) since they remain as σ^* orbitals. The t_{2g} set, however, would split substantially into a nonbonding b_{2g} (d_{xy}) orbital and a π antibonding e_g (d_{xz}, d_{yz}) pair of orbitals as the results of π interaction between the metal d_π orbitals and the p_π orbitals of the axial ligands. We expect a closed-shell electronic configuration with the HOMO to be the doubly occupied d_{xy} orbital and the LUMO to be the degenerate π^* orbital. Above the LUMO should be the σ antibonding orbitals, namely, $d_{x^2-y^2}$, and d_{z^2}. In D_{4h} symmetry, a linear combination of four chalcogen p_π orbitals gives rise to two doubly degenerate orbitals, namely, e_g and e_u, but only the e_g orbital interacts with the metal d_π orbitals also of e_g symmetry, and the e_u orbital that remains may be described as a degenerate p_π lone pair orbital. Therefore, in addition to the M−Q σ bonds, there are also two π bonds, and hence a double bond between the metal atom and each of the chalcogen atoms.

The above description of the electronic structure can be developed more quantitatively by the previously reported DV−Xα calculations on $W(Q)_2(PH_3)_4$ (Q = O, S, Te)[9] and our Xα-SW calculation on the $Mo(S)_2(PH_3)_4$ complex. Shown in Figure 2 are the upper valence Xα−SW MOs of $Mo(S)_2(PH_3)_4$ in D_{2h} symmetry together with approximately placed metal d_π orbitals and sulfur p orbitals. In examining this diagram, note that upon lowering molecular symmetry from D_{4h} to D_{2h}, the orbital symmetries correlate as follows: $a_{1g} \rightarrow a_g$, $b_{2g} \rightarrow a_g$, $e_g \rightarrow b_{2g}$ and b_{3g}, and $e_u \rightarrow b_{2u}$ and b_{3u}.

As would be expected, the MO diagram in Figure 2 shows a well-defined closed-shell configuration in which the nonbonding

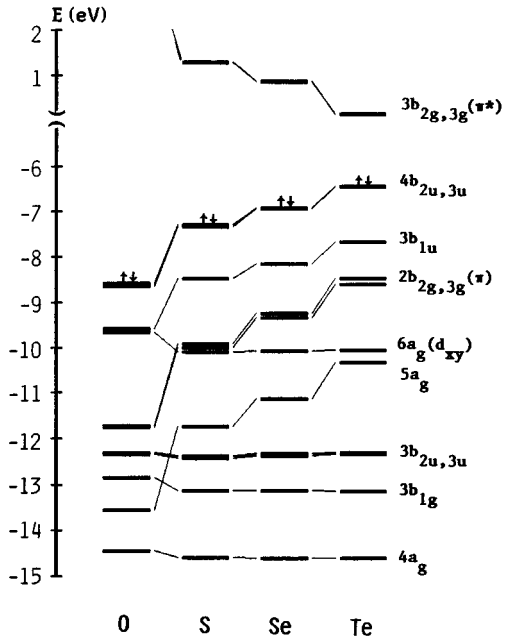

Figure 3. Upper valence molecular orbitals for $Mo(Q)_2(PH_3)_4$ (Q = O, S, Se, and Te) calculated by the *ab initio* RHF method with ECP approximation.

d_{xy} ($6a_g$) orbital is the HOMO, and, therefore, the ground state of these molecules is a closed-shell singlet state, ^1A_g. The LUMO is, also as expected, the π^* or the $3b_{2g}$ (d_{xz}) and $3b_{3g}$ (d_{yz}) orbitals. The lowest energy bands in the absorption spectra of such complexes have been assigned accordingly to the transition from the nonbonding d_{xy} orbital to the π^* orbitals.[3,8] Other Mo−S bonding orbitals shown in Figure 2 are the π-bonding $2b_{2g}$ and $2b_{3g}$ orbitals and the σ-bonding $5a_g$ orbital. The Mo−P bonding can be attributed mainly to the low-lying $4a_g$, $3b_{1g}$, $3b_{2u}$, and $3b_{3u}$ orbitals in which the $3b_{1g}$ orbital has a contribution from the metal $d_{x^2-y^2}$ orbital. Below the HOMO, the $4b_{2u}$ and $4b_{3u}$ orbitals are simply the sulfur p_π lone pair orbitals, and the $3b_{1u}$ orbital is largely an out-of-phase combination of the p_z orbitals of the S atoms but with a small contribution from the metal p orbital which leads to a little Mo−S σ bonding character. In the following we will simply refer to this orbital as the p_z lone pair orbital.

Let us now turn to the ground state electronic structures given by the *ab initio* RHF calculations. We display in Figure 3 again the upper valence MOs from such calculations with the ECP approximation for $Mo(Q)_2(PH_3)_4$ with Q = O, S, Se, and Te. The characters of each orbital in Figure 3 are essentially the same as those of the Xα orbitals of the same label in Figure 2. For example, the $4b_{2u}$ and $4b_{3u}$ orbitals in both cases are the p_π lone pairs on the chalcogen atoms. Moreover, the same orbitals are occupied in both *ab initio* and Xα calculations. Therefore, our previous discussion of bonding should still be applicable, and we have the same closed-shell ground state electronic configuration. However, there is a striking difference in the electronic structures given by the two types of calculations.

As shown in Figure 3 the HOMO in the *ab initio* MO diagram for each complex is *not* the expected nonbonding metal d_{xy} orbital, but the chalcogen p_π lone pair orbitals. This difference then raises an important question about previous assignments of the electronic absorption spectra in terms of MO diagrams which make the d_{xy} orbital the HOMO. We will return to this question shortly.

It should be mentioned that the same results as those in Figure 3 were also obtained from all-electron *ab initio* RHF calculations employing large basis sets on $Mo(O)_2(PH_3)_4$ and $Mo(S)_2(PH_3)_4$.

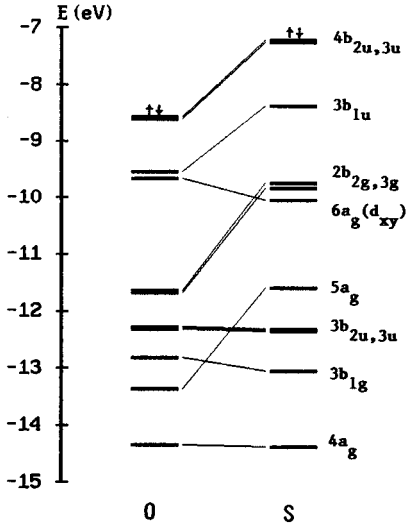

Figure 4. Upper valence molecular orbitals for $Mo(Q)_2(PH_3)_4$ (Q = O and S) calculated by the all-electron *ab initio* RHF method.

The MO diagrams from the all-electron calculations are shown in Figure 4. By comparing Figure 4 with the first two columns of Figure 3 which are obtained with the ECP approximation, it is clear that the MO diagrams obtained by the two types of calculation are almost identical.

A trend in the metal−chalcogen interaction can be clearly seen from Figure 3. The energies of both metal−chalcogen σ ($5a_g$) and π ($2b_{2g}$ and $2b_{3g}$) bonding orbitals drop significantly together with destabilization of their antibonding counterparts as we go from Q = Te to Q = O. On the other hand, decreasing energy of the chalcogen lone pair orbitals ($3b_{1u}$, $4b_{2u}$, and $4b_{3u}$) in the same order is consistent with the ordering of the p orbital energies of the chalcogen atoms. The change of the orbital energies is rather smooth from Q = Te to Q = S, but there is a clear and sudden jump from Q = S to Q = O, and the π^* orbitals ($3b_{2g}$ and $3b_{3g}$) in the oxo compound are so high (4eV) that it was impractical to include them in the figure. There is thus a significant difference between the oxo compound and other members of the family. It is interesting to note in Figure 3 that the energies of the Mo−P bonding orbitals ($4a_g$, $3b_{1g}$, $3b_{2u}$ and $3b_{3u}$) as well as the nonbonding d_{xy} orbital change very little across the series of four complexes, that is, even including the oxo compound. It can thus be concluded that the Mo−P bonding is largely independent of the Mo−chalcogen bonding.

Finally, the ground states of all these compounds were also calculated by the CASSCF method. The dominant configuration in the CASSCF wave function is just the closed-shell HF configuration with coefficients of 0.91, 0.90, 0.88, and 0.86 for the O, S, Se, and Te complexes, respectively. The CASSCF wave functions were constructed by distributing 14 electrons in a set of 11 active orbitals. The active orbital space (see also Figure 3) consists of the metal−chalcogen bonding orbitals ($5a_g$, $2b_{2g}$ and $2b_{3g}$), the metal nonbonding orbital ($6a_g$), the chalcogen lone pair orbitals ($3b_{1u}$, $4b_{2u}$ and $4b_{3u}$), the metal−chalcogen π^* orbitals ($3b_{2g}$ and $3b_{3g}$), and the metal−chalcogen and Mo−P σ^* orbitals (d_{z^2} and $d_{x^2-y^2}$), not shown in either Figure 2 or Figure 3 because of their high energies. The same orbital space was also used in the CASSCF calculations of excited states as discussed below. In addition, the $Mo(S)_2(PH_3)_4$ compound was also calculated with a larger CASSCF active space (16 electrons in 14 orbitals). It was obtained by adding one occupied orbital (the $3b_{1g}$ Mo−P bonding orbital) and two empty orbitals of a_g and b_{1u} symmetries to the active orbital set described earlier.

Electronic Transitions in $Mo(S)_2(PH_3)_4$, $Mo(Se)_2(PH_3)_4$, and $Mo(Te)_2(PH_3)_4$. We now turn to the electronic transitions

in these three complexes. The absorption spectra of the Mo(Q)$_2$(dppee)$_2$ (Q = O, S, Se,Te) compounds have all been measured in this laboratory.[12] The spectrum of the oxo complex will be considered separately because some features there are very different. The low-energy absorptions in the spectra of the Mo(Q)$_2$(dppee)$_2$ (Q = S, Se, Te) compounds appear to be simple, clear, and very consistent. In all three cases, the lowest absorption is characterized by a very weak, broad band centered around 550, 640, and 770 nm for Q = S, Se, and Te, respectively. Following this, there are either two absorptions of similar energies or one absorption in the spectrum of each of these compounds. The absorptions are relatively weak, and they are two shoulders at 425 and 415 nm for Q = S, two bands at 585 and 520 nm for Q = Se, and one band at 625 nm for Q = Te. Finally, in the low-energy region, each of the three spectra is also characterized by a very strong absorption band. The peaks of these bands are located at 375, 415, and 485 nm, respectively, for Q = S, Se, and Te. These strong bonds are three orders of magnitude stronger than the lowest-energy bonds. The spectrum of a tellurido complex of molybdenum is also known for Mo(Te)$_2$(PMe$_3$)$_4$,[7] but only one dominant strong band at 488 nm has been reported there.

Assignment of the measured spectra did not seem to be a problem before. Justified by the ligand-field theory or Xα MO calculations, the lowest energy bands which are also very weak in the spectra of dioxo rhenium complexes[3] and chalcogenido tungsten complexes[8,9] had always been assigned to the ligand-field transitions, namely, transitions from the nonbonding metal d_{xy} orbital (the HOMO) to the metal−chalcogen π^* orbitals (the LUMO). Following the same argument, the absorptions at 550, 640, and 770 nm in the spectra of Mo(Q)$_2$(dppee)$_2$, Q = S, Se, Te, respectively, would have been given the same assignment according to the MO diagrams in Figure 2. However, these absorptions could also be assigned to transitions of a totally different nature, if we choose to consider the spectra in terms of the MO diagrams in Figure 3 obtained from the *ab initio* calculations in which the HOMO is the chalcogen p_π lone pair orbitals and the d_{xy} orbital has much lower energy. In the present theoretical study of the absorption spectra, we do not rely on either of those MO diagrams, though they will be mentioned. We calculated energies of electronic transitions by carrying out CASSCF or full-CI calculations on the ground state and various low-lying excited states. The results of these calculations are summarized in Table 1. The results for Mo(S)$_2$(PH$_3$)$_4$ calculated with the larger active space are listed in parentheses. As can be seen, there are not any qualitative differences between the results given by the CASSCF calculations of different sizes.

The calculated excited states for Mo(Q)$_2$(PH$_3$)$_4$ (Q = S, Se, Te) may be divided into four blocks as shown in Table 1 according to their energies relative to the ground state (^1A_g) and their origins. The lowest excited states in the first block are those due to excitations of an electron from the chalcogen p_π lone pair orbitals ($4b_{2u}$ and $4b_{3u}$, Figure 3) to the π^* orbitals ($3b_{2g}$ and $3b_{3g}$), or the $p_\pi \rightarrow \pi^*$ transitions. The first excited state is the triplet $^3B_{1u}$ state in all three complexes. In the energy range of the first block, we also have two triplet states, $^3B_{2g}$ and $^3B_{3g}$, that are from excitations out of the nonbonding d_{xy} orbital ($6a_g$) to the π^* orbitals.

As can be seen in Table 1, the calculated relative energies of the excited states in the first block for Mo(S)$_2$(PH$_3$)$_4$ and Mo(Se)$_2$(PH$_3$)$_4$ are all close to the observed values of the first absorption bands. Therefore, based on the matching energies, we think that this first band in both cases should be mainly assigned to the singlet-singlet $p_\pi \rightarrow \pi^*$ transitions. It may be noted that a transition from the ligand p_π lone pair orbital to the mainly metal based π^* orbital is clearly different in nature from a usually intense $\pi \rightarrow \pi^*$ transition, for example, in an organic system. The $p_\pi \rightarrow \pi^*$ transitions may not have to be intense at all even though they involve an allowed ^1A_g to $^1B_{1u}$ transition. The calculated results also suggest that there may be several transitions possible in the energy range, which is consistent with the observation that the first absorption in the spectra of Mo(S)$_2$(dppee)$_2$ and Mo(Se)$_2$(dppee)$_2$ is a broad band without a clear peak. As a matter of fact, in the well-resolved spectra of W(Te)$_2$(PMe$_3$)$_4$,[8] three lowest absorption bands can be seen clearly in a close energy range. Similarly, the lowest absorption (770 nm) in the spectrum of Mo(Te)$_2$(dppee)$_2$ may also be assigned to the $p_\pi \rightarrow \pi^*$ transitions, even though the calculated energies for Mo(Te)$_2$(PH$_3$)$_4$ in the first block of Table 1 are all lower than the observed value.

Table 1. Electronic Transition Energies in Mo(Q)$_2$(PH$_3$)$_4$ (Q = S, Se, Te)

		energy, nm					
		Mo(S)$_2$(PH$_3$)$_4$		Mo(Se)$_2$(PH$_3$)$_4$		Mo(Te)$_2$(PH$_3$)$_4$	
transition	origin	calcd	exptl[a]	calcd	exptl[b]	calcd	exptl[c]
$^3B_{1u} \leftarrow {}^1A_g$	$p_\pi \rightarrow \pi^*$	594	748			1028	
^3A_u		557	705			960	
^3A_u		493		614		848	
^1A_u	$p_\pi \rightarrow \pi^*$	547 (559)[d]	550	701	640	971	770
$^1B_{1u}$		530		676		941	
^1A_u		471		597		828	
$^3B_{2g}$	$d_{xy} \rightarrow \pi^*$	544		654		833	
$^3B_{3g}$		545		654		830	
$^3B_{2u}$	$p_z \rightarrow \pi^*$	466		522		618	
$^3B_{3u}$		464		518		612	
$^1B_{3g}$	$d_{xy} \rightarrow \pi^*$	432 (421)	425	499	585	609	625
$^1B_{2g}$		431 (421)	415	498	520	608	
$^1B_{2u}$	$p_z \rightarrow \pi^*$	429 (395)	375	481	415	565	485
$^1B_{3u}$		426 (393)		477		559	
$^3B_{1g}$	$d_{xy} \rightarrow d_{x^2-y^2}$	443		418		436	
$^1B_{1g}$		360		373		345	
$^1B_{1g}$	$\pi \rightarrow \pi^*$	279		350		468	
$^1B_{1g}$		275		339		418	
^1A_g		273		331		423	

[a] Measured for *trans*-Mo(S)$_2$(dppee)$_2$.[12] [b] Measured for *trans*-Mo(Se)$_2$(dppee)$_2$.[12] [c] Measured for *trans*-Mo(Te)$_2$(dppee)$_4$.[12] [d] Results in parentheses are obtained with the larger CASSCF active space.

The second block in Table 1 consists of triplet components of transitions from the chalcogen p_z lone pair orbital ($3b_{1u}$, Figure 3) to the π^* orbitals, $p_z \rightarrow \pi^*$, and the singlet-singlet $d_{xy} \rightarrow \pi^*$ transitions or the ligand-field transitions. The calculated energies of these transitions well match the observed values at 425 and 415 nm for Mo(S)$_2$(dppee)$_2$, at 585 and 520 nm for Mo(Se)$_2$(dppee)$_2$, and at 625 nm for Mo(Te)$_2$(dppee)$_2$. We then assign these observed weak absorptions to the dipole-forbidden but spin-allowed singlet $d_{xy} \rightarrow \pi^*$ transitions, namely, $^1B_{3g} \leftarrow {}^1A_g$ and $^1B_{2g} \leftarrow {}^1A_g$. Our CASSCF calculations thus predict that the so-called ligand-field transitions are not the lowest energy transitions in this class of compounds. Such transitions should occur with higher energies than the transitions from the p_π lone pairs of the chalcogen atoms to the π^* orbitals.

We chose in the calculations the angle P−Mo−P to be 90° so that the molecules in Figure 1 have a virtual D_{4h} symmetry if one neglects the hydrogen atoms in PH$_3$. Because of this, the π^* orbitals ($3b_{2g}$ and $3b_{3g}$, Figure 3) are almost degenerate and, therefore, the calculated energies for the $^1B_{2g}$ and $^1B_{3g}$ excited states are also almost the same as shown in Table 1. By reduction of the angle to a value a little less than 90° as in the real cases with the dppee ligand, the energies of these excited states would certainly split. Such a split, however, may not

necessarily be significant as shown in the case of the sulfido complex or the tellurido complex where only one band is observed.

The calculated electronic transitions listed in the third block of Table 1 are the $^1B_{2u}\leftarrow{}^1A_g$ and $^1B_{3u}\leftarrow{}^1A_g$ transitions which are both dipole- and spin-allowed. As indicated in the table, they originate from exciting an electron from the p_z lone pair orbitals of the chalcogen atoms to the π^* orbitals. Since the absorption next in line in the measured spectrum of each of the three complexes is a very strong band, we may then very reasonably assign this absorption band to the singlet $p_z\rightarrow\pi^*$ transitions.

A similar series of such strong bands in the spectra of $W(Q)_2(PMe_3)_4$ (Q = S, Se, Te) has been assigned to a $\pi\rightarrow\pi^*$ transition.[8] Our calculations indicate that the $\pi\rightarrow\pi^*$ transitions should occur at higher energies than the $p_z\rightarrow\pi^*$ transitions. This is shown in the last block of Table 1 by three singlet−singlet transitions from the ground state to the excited states arising from the $\pi\rightarrow\pi^*$ excitations. In D_{2h} symmetry, the $\pi\rightarrow\pi^*$ excitations give rise to four singlet excited states, namely, two ^1A_g and two $^1B_{1g}$ states. Three of these were found to have similar lower energies and are listed in Table 1. Also included in this last block is the $d_{xy}\rightarrow d_{x^2-y^2}$ transition. It is interesting to note that the calculated energy for this transition is essentially unchanged from Q = S to Q = Te, whereas all other transitions move to lower energies in the series Q = S, Se, and Te. The change in the transition energies on moving to the heavier chalcogen atoms correlates well with changes in orbital energy differences. For example, the decreasing energies of the $\pi\rightarrow\pi^*$ transitions from $Mo(S)_2(PH_3)_4$ to $Mo(Te)_2(PH_3)_4$ correspond directly to the narrowing energy gap between the π and π^* orbitals in Figure 3.

Our discussion of the electronic spectra for the molybdenum complexes may also be applied to the spectra of the tungsten complexes, $W(Q)_2(PMe_3)_4$ (Q = S, Se, Te).[8] In the reported spectra of these complexes the low-energy absorption bands may also be roughly divided into three groups, namely, two or three absorptions that are closely spaced and of low intensity in the lowest energy region, one or two absorptions at higher energies, and then a very strong band at even higher energy. Figure 5 shows the *ab initio* RHF MO diagrams for $W(S)_2(PH_3)_4$ and $W(Te)_2(PH_3)_4$. Since they were calculated in D_{2d} symmetry, the MOs in the figure have been labeled accordingly. Comparing the diagrams in Figure 5 with those in Figure 3 for the corresponding molybdenum compounds, we see the similarity immediately.

Electronic Transitions in $Mo(O)_2(PH_3)_4$. The electronic absorption spectrum of the $Mo(O)_2(dppee)_2$ complex is very different from the spectra of $Mo(Q)_2(dppee)_2$ (Q = S, Se, Te). Below 300 nm there are only two weak shoulders, at 435 and 480 nm, in the spectrum of $Mo(O)_2(dppee)_2$.[12] Interestingly, the features of the spectrum of the oxo compound were very well predicted by our calculations before any measurement was made.

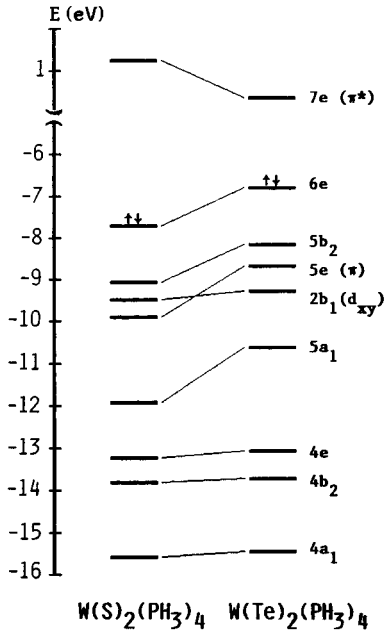

Figure 5. Upper valence molecular orbitals for $W(Q)_2(PH_3)_4$ (Q = S and Te) calculated by the *ab initio* RHF method with ECP approximation.

As noted earlier, the ground state electronic structure of $Mo(O)_2(PH_3)_4$ is markedly different from those of the other members of the molybdenum chalcogenide family. In the MO diagrams in Figure 3, the differences are highlighted by the much stabilized Mo−O σ and π bonding orbitals and their much destabilized antibonding counterparts and also by the low-energy p_π lone pair orbitals. Any electronic transitions from a bonding, nonbonding, or lone pair orbital to the Mo−O antibonding orbitals would certainly be expected to have much higher energy than those of the same transitions in Table 1, which is confirmed by the results of the CASSCF calculations. For $Mo(O)_2(PH_3)_4$, the same excited states as those listed in Table 1 were again calculated. It was found that all electronic transitions that may be designated as the $p_\pi\rightarrow\pi^*$, $d_{xy}\rightarrow\pi^*$, $p_z\rightarrow\pi^*$, and $\pi\rightarrow\pi^*$ transitions have energies over 330 nm. The only transitions that have energies below 330 nm are those of $^1B_{1g}\leftarrow{}^1A_g$ and $^3B_{1g}\leftarrow{}^1A_g$ at 383 and 465 nm, respectively, which are the singlet and triplet components of the $d_{xy}\rightarrow d_{x^2-y^2}$ excitation. Since we lack an alternative, the observed absorptions (shoulders at 435 and 480 nm) may then be necessarily assigned to these transitions.

Acknowledgment. We thank the National Science Foundation for support and the Department of Chemistry and the Supercomputer Center at Texas A&M University for computer time. We are grateful to Professor M. B. Hall for access to the GAMESS program package.

IC951261Q